第 29 卷第 10 期 无 机 化 学 学 报 Vol.29 No.10
2013 年 10 月 CHINESE JOURNAL OF INORGANIC CHEMISTRY 2231-2238

碳酸铵水解法制备耐高温介孔 CeO_2 材料

陈山虎 曹 毅 兰 丽 赵 明 史忠华* 龚茂初 陈耀强
(四川大学化学学院, 绿色化学与技术教育部重点实验室,成都 610064)

摘要: 以 H_2O_2 为氧化剂,分别以传统沉淀法(以氨水为沉淀剂)和碳酸铵水解法制备了 CeO_2 材料。采用傅里叶变换红外(FTIR)、拉曼光谱(Raman)、热重–差示扫描分析(TG-DTA)及 X 光电子能谱(XPS)等手段对沉淀前躯体及其分解过程进行了研究。结果表明,在碳酸铵水解法制备的前躯体中含有 O_2^{2-},CO_3^{2-}和 OH^-物种,而在水解过程中,碳酸根会逐渐被氢氧根取代。虽然两者方法制备的沉淀的化学成分基本一样,但碳酸铵水解法改变了沉淀颗粒的堆积方式,因此制备的 CeO_2 具有更好的抗高温老化性能和还原性能。经过 900 ℃焙烧 3 h 后,比表面仍有 27 $m^2 \cdot g^{-1}$。

关键词: 水解法; 传统沉淀法; 耐高温; 氧化还原性能
中图分类号: O614.33+2 **文献标识码**: A **文章编号**: 1001-4861(2013)10-2231-08
DOI:10.3969/j.issn.1001-4861.2013.00.219

Preparation of Mesoporous CeO_2 with High Thermal Stability by Ammonium Carbonate Hydrolysis Method

CHEN Shan-Hu CAO Yi LAN Li ZHAO Ming
SHI Zhong-Hua* GONG Mao-Chu CHEN Yao-Qiang
(*Key Laboratory of Green Chemistry and Technology of the Ministry of Education, College of Chemistry, Sichuan University, Chengdu* 610064, *China*)

Abstract: Two series of CeO_2 materials were prepared by two different synthetic routes, i.e. the conventional ammonia precipitation route (CR) and the ammonium carbonate hydrolysis route (HA) using $(NH_4)_2CO_3$ in the presence of hydrogen peroxide. The formation process and decomposition behavior of the precipitates were investigated by FTIR, Raman, thermogravimetric and differential thermal analysis (TG/DTA) and X-ray photoelectron spectroscopy (XPS). The results show that the as-prepared precipitate obtained by HA consists of O_2^{2-}, CO_3^{2-} and OH^- species. However, after hydrothermal digestion at 80 ℃, the CO_3^{2-} species is gradually hydrolyzed into OH^- species. Although the chemical components of the digested precipitates prepared by these two routes are almost the same, the agglomeration of CeO_2 particles is markedly modified. The CeO_2 powder produced by HA exhibits higher thermal stability and better reduction property compared to that obtained by CR. After the heat treatment at 900 ℃ for 3 h, the CeO_2 powder from HA route still remains a surface area of 27 $m^2 \cdot g^{-1}$.

Key words: hydrolysis method; conventional precipitation; high thermal stability; redox properties

CeO_2 has attracted much attention in recent years for its applications in many commercial processes, such as catalytic wet oxidation[1], soot combustion[2], and fuel cell technology[3]. Moreover, CeO_2 has also been widely utilized as oxygen storage material in three way catalysts (TWCs) for the purification of

收稿日期:2013-01-07。收修改稿日期:2013-03-19。
国家自然科学基金(No.20803049,21173153)资助项目。
*通讯联系人。E-mail:shizh96@scu.edu.cn;会员登记号:S06N7858M1007。

exhaust gases from automobile engines[4]. CeO_2 can act as an oxygen buffer by releasing and storing oxygen under rich and lean conditions, respectively, involving the Ce^{4+}/Ce^{3+} couple. This ensures that the air to fuel ratio is kept around the stoichiometric point (14.6), which is crucial to maintain the efficiency of TWCs[5]. In addition, multiple functions are also associated with CeO_2: stabilization of noble metal dispersion and Al_2O_3 support, promotion of water-gas shift reaction, and enhancement of CO oxidation[4,6-9].

For application as an oxygen storage material in TWCs, high surface area is preferred. However, pure CeO_2 is thermally unstable. For instance, after calcination at 850 ℃, the surface area of CeO_2 sample is only 5 $m^2 \cdot g^{-1}$ [10]. The loss of surface area will cause the deterioration of oxygen storage and release properties. Therefore, thermal stability is one of the most important properties.

In attempt to get CeO_2-based materials with high thermal resistance, numerous approaches, including precipitation method[11-12], hydrothermal route[13-15], sol-gel techniques[16-18], surfactant-assisted approach[19-21] and combustion synthesis[22-23], have been developed to produce CeO_2 material. Up to now, the most convenient method is precipitation, wherein the precursors of cerium mainly include Ce(Ⅲ) and Ce(Ⅳ), while ammonia is conventionally used as the base. In this method, the H_2O_2-assisted route developed by Woodhead[24] has been investigated extensively. Under basic condition, Ce(Ⅲ) can be oxidized into Ce(Ⅳ), in the form of $Ce(OH)_4$ or $CeO_2(OH)_2$, which will be converted into CeO_2 by the following hydrolysis and thermal decomposition processes[25-26]. However, to the best of our knowledge, there have been no open reports on the investigation of this method employing ammonium carbonate as the precipitant.

In this study, we have developed an ammonium carbonate hydrolysis route based on the H_2O_2-assisted method, aiming at producing CeO_2 material with higher thermal stability. In particular, the formation mechanism for the precipitate has also been examined. The textural and structural properties of CeO_2 oxide are influenced by the precursors. In the ammonium carbonate environment, the growth process as well as the agglomeration of CeO_2 particles is controlled, which enlarges the grain size of CeO_2 and facilitates the improvement of thermal stability and reduction property[27].

1 Experimental

1.1 Synthesis

1.1.1 Preparation of undigested precipitates

A solution was prepared by dissolving $Ce(NO_3)_3 \cdot 6H_2O$ in distilled water, then a freshly standardized H_2O_2 solution (30wt%) was added. The molar ratio of $Ce(NO_3)_3$:H_2O_2 was 1:1.5. An ammonium carbonate solution (25wt%) was added into the salt solution, under stirring, until pH=8.5. The obtained precipitate was filtered, washed with distilled water until constant pH value, and air-dried at room temperature to obtain CeO_2-H. For comparison, an ammonia solution (25wt%) was also used to prepare CeO_2 precursor following the same procedure, and the obtained sample was labeled as CeO_2-C.

1.1.2 Preparation of digested precipitates

An ammonium carbonate solution (25wt%) was added into the mixed solution of $Ce(NO_3)_3 \cdot 6H_2O$ and H_2O_2 (the molar ratio of $Ce(NO_3)_3$:H_2O_2 was 1:1.5), under stirring until the pH value of 8.5. The reaction vessel was placed in a water bath, and the solution was heated at 80 ℃ for 12 h, under vigorous stirring. The precipitate was filtered, washed with distilled water, and dried at 70 ℃ for 5 h to obtain sample CeO_2-H80. In addition, another sample (CeO_2-C80) was also made under the same condition except that ammonia was employed as the precipitant.

1.1.3 Calcination of precipitates

The CeO_2-H80 and CeO_2-C80 samples were further calcined at different temperatures in the range of 500~900 ℃ for 3 h. The obtained oxides were labeled as CeO_2-H*t* and CeO_2-C*t*, respectively, where *t* represents the calcination temperature.

1.2 Characterizations

The FTIR measurements were performed on a Nicolet 6700 FT spectrometer, working in the range of 400~4 000 cm^{-1} at a resolution of 4 cm^{-1} using KBr

pellet.

The precipitate was analyzed by Raman spectroscopy using a LabRAM HR800 with confocal microscope system. The specimen was illuminated through a 50×objective with 633 nm excitation from a diode laser source at a laser power of 150 mW and with a spot size of 3 μm. Raman spectra were collected in the range of 200~2 000 cm^{-1}.

X-ray photoelectron spectra were obtained on a XSAM 800 spectrometer (KRATOS Corp.), employing Mg $K\alpha$ radiation ($h\nu$=1 253.6 eV) and working at 13 kV and 20 mA. The C1*s* peak (284.6 eV) was used to calibrate the binding energy.

The weight loss and thermal behavior of the sample were examined by a HCT-2 analyzer (Beijing Science Apparatus Factory, Beijing, China) in flowing nitrogen atmosphere. The sample was heated to 600 ℃ at a heating rate of 10 ℃·min^{-1}.

The textural properties were determined by N_2 adsorption-desorption method on a Quantachrome SI instrument. The specific surface area and pore size distribution of the sample were obtained according to Brunauer-Emmett-Teller (BET) method and Barret-Joyner-Halenda (BJH) equation, respectively. Prior to each measurement, the sample was degassed at 300 ℃ for 3 h under vacuum.

X-ray diffraction patterns were recorded using a D/max-rA diffractometer (RIGAKU Corp.) with Cu $K\alpha$ radiation (40 kV, 25 mA, λ=0.154 18 nm). The crystal size was calculated by Scherrer′s equation using the data of (111) peak.

Temperature-programmed reduction (TPR) was determined in a conventional reactor equipped with a thermal conductivity detector. Prior to the analysis, the sample (100 mg) was cleaned by flowing N_2 at 450 ℃ for 45 min. The measurement was performed from room temperature to 900 ℃ in a flow of 5% H_2/N_2(*V*/*V*) (20 mL·min^{-1}) at a heating rate of 10 ℃·min^{-1}.

2　Results and discussion

2.1　Formation processes of the precipitates

Composition of the precipitate depends on the kind of cations and anions in the solution. In the present work, Ce^{3+} is employed as cerium precursor, while OH^- or CO_3^{2-} is used as the precipitant, in the presence of hydrogen peroxide[28].

When ammonia is utilized as the precipitant, the following equations are expected during the precipitation and digestion processes[25]:

$$Ce^{3+}+(3/2)H_2O_2+3OH^- \rightarrow Ce(O_2)(OH)_2+2H_2O \quad (1)$$

$$Ce(O_2)(OH)_2 \rightarrow CeO_2+(1/2)O_2+H_2O \quad (2)$$

The proposed mechanism of ammonium carbonate hydrolysis route is as follows[25-26,29]:

$$CO_3^{2-}+H_2O \rightarrow HCO_3^-+OH^- \quad (3)$$

$$Ce^{3+}+(3/2)H_2O_2+OH^- \rightarrow Ce(O_2)^{2+}+2H_2O \quad (4)$$

$$Ce(O_2)^{2+}+OH^-/CO_3^{2-} \rightarrow Ce(O_2)(OH)_x(CO_3)_{1-x/2} \quad (5)$$

During the heating process of the solution at 80 ℃, CeO_2 is gradually formed via:

$$Ce(O_2)(OH)_x(CO_3)_{1-x/2}+H_2O \rightarrow Ce(O_2)(OH)_2+CO_2 \quad (6)$$

$$Ce(O_2)(OH)_2 \rightarrow CeO_2+(1/2)O_2+H_2O \quad (7)$$

The dehydration behavior may take place during the whole operation process because the O_2^{2-} and OH^- groups are not stable[25,30].

Fig.1 shows the FTIR spectra of the precipitates before and after heat treatment at 80 ℃. The intense and broad bands in the 3 000~3 750 cm^{-1} region are normally ascribed to the stretching of surface hydroxyl groups or molecularly chemisorbed H_2O[28,31-32]. Obviously, three distinguished signals are observed, indicating the coexistence of mono-coordinated, bi-coordinated and tri-coordinated hydroxyl groups[28,31-32]. The relative intensity of this region for CeO_2-H becomes stronger after digestion, whereas CeO_2-C shows a different trend. This reveals that the carbonate species is hydrolyzed into hydroxyl groups during the digestion process. The minor band at 2 300~2 400 cm^{-1} corresponds to the coordinated CO_2 adsorbed at the surface, while the feature at ~1 620 cm^{-1} is assigned to the adsorption of H_2O[28,33]. Several adsorption bands around 1 620, 1 380, 1 136, 1 030 and 913 cm^{-1} are associated with the carbonate species[32,34-35]. Among these bands, the one around 1380 cm^{-1} is probably assigned to the carbonate species from the ammonium carbonate precipitator because it can only be observed in CeO_2-H, whilst the others are likely caused by atmospheric dioxide[36].

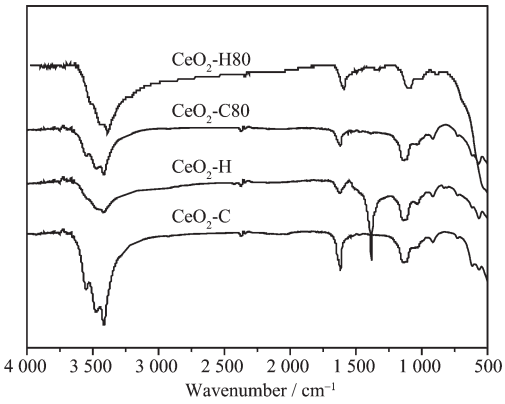

Fig.1 FTIR spectra of precipitates

Raman spectra of the precipitates are presented in Fig.2. It has been reported that bulk CeO_2 shows a strong peak centered at 456 cm^{-1} or 471 cm^{-1} corresponding to the symmetric breathing mode of the O^{2-} anions [26,37]. However, both of the peaks can be found in this work. The broad peak around 608 cm^{-1} is ascribed to the defect site of CeO_2 crystallite, which seems to be caused by the influence of H_2O_2 [26]. The formation of CeO_2 suggests that the following overall process has occurred[25]:

$$Ce^{3+}+(3/2)H_2O_2+3OH^- \rightarrow CeO_2+(1/2)O_2+3H_2O \quad (\mathbf{8})$$

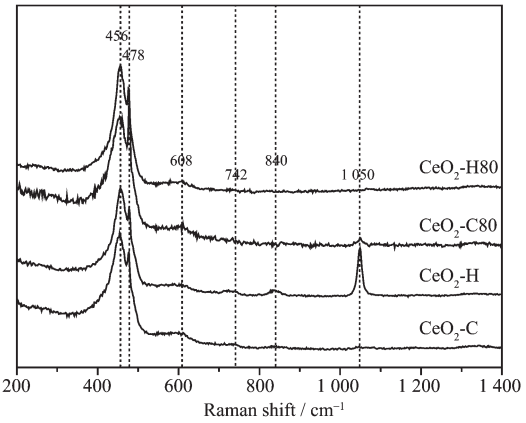

Fig.2 Raman spectra of precipitates

Three bands, locating at about 742, 1 050 and 1 350 cm^{-1}, respectively, are likely related to the CO_3^{2-} species[26]. Notably, these spectral features for CeO_2-H are the strongest among the samples because of the usage of ammonium carbonate. The reduction of the bands for CeO_2-H80 compared to CeO_2-H implies that the CO_3^{2-} species is hydrolyzed during digestion process, in accordance with TG-DTA and IR results. An additional weak band at about 840 cm^{-1} can be observed in the spectra for CeO_2-C and CeO_2-H, which is indicative of the O-O stretching vibration of η^2-peroxide (O_2^{2-}) species[38], indicating the formation of CeO_2^{2+} precursors. However, the band vanishes after digestion. This implies that the O_2^{2-} species is more or less eliminated during the thermal treatment, because the O_2^{2-}-containing species is not stable[25-26]. The Raman results confirm the occurrence of Eqs.(**3**)~(**7**).

The oxidation states of cerium for the precipitates prepared by different routes are shown in Fig.3. The spectra are very similar, showing six peaks at around 883.0, 888.9, 898.5, 901.1, 907.4, and 916.8 eV, respectively. All the spectra are attributed to the diversified states of Ce^{4+} and no signals related to Ce^{3+} are found [39], from which we can conclude that Ce(Ⅲ) is fully oxidized into Ce (Ⅳ) by H_2O_2 under basic condition.

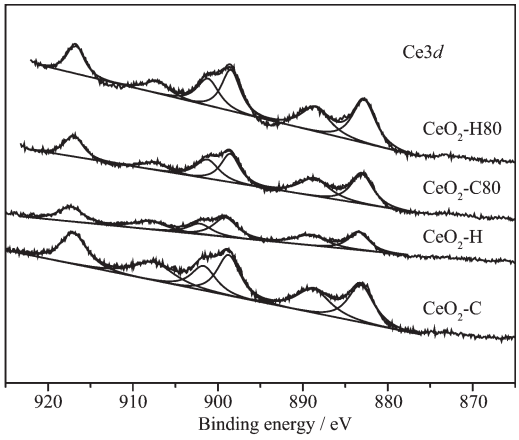

Fig.3 Ce3*d* XPS spectra for precipitates

The O1*s* spectra are shown in Fig.4. The peak at about 529.7 eV is characteristic of the O^{2-} anions in bulk CeO_2[39], while the peaks at 531.5 and 532.7 eV correspond to OH^- and CO_3^{2-} species, respectively[40-41]. It is obvious that the contents of OH^- and CO_3^{2-} species for the digested precipitates are lower than those of the undigested ones, due to the fact that the hydrolysis of CO_3^{2-} species as well as the dehydration of OH^- species takes place during digestion. The relative contents of Ce, O and C are calculated. The relative contents of atoms in CeO_2-C are different from CeO_2-H. The content of C of CeO_2-H is much higher than that of CeO_2-C due to the participation of CO_3^{2-} species during the precipitation procedure. However,

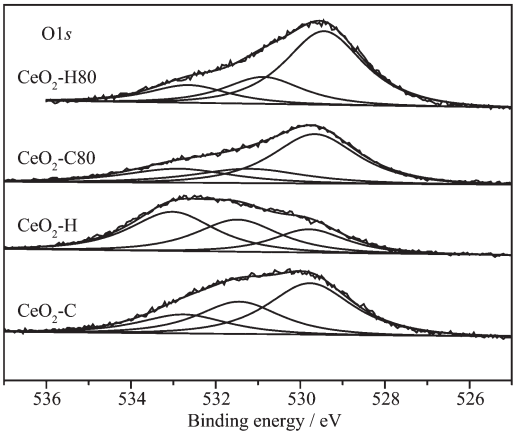

Fig.4　O1*s* XPS spectra for precipitates

the amount of the elements for CeO_2-C80 and CeO_2-H80 is almost the same, providing another evidence for the occurrence of equation (6) for CeO_2-H. It is important to remark that the C element is difficult to evaluate due to the interference of adventitious carbon and physically absorbed CO_2[26].

Fig.5 displays the TG/DTA curves of the precipitates. Both of the precipitates prepared by ammonia show a steady decomposition process, regardless of digestion. For CeO_2-C, the total weight loss is about 20.3%, which is much higher than that of CeO_2-C80 (13.4%), indicating that the dehydration process, i.e., equation (**2**), has occurred during the heat treatment at 80 ℃[30]. The DTA curve shows one endothermic peak below 100 ℃, which is probably ascribed to the elimination of surface physical-adsorbed water[30]. Since the decomposition process of $Ce(O_2)(OH)_2$ is a slow and successive process, no obvious exothermal phenomena can be observed. The weight loss procedure of CeO_2-H shows complex stages, approximately locating at the temperature ranges of 25~200 ℃, 250~350 ℃ and 350~450 ℃, respectively. The first region appears as a result of the elimination of physically adsorbed water and the decomposition of O_2^{2-} and hydroxyl groups[25,28,30]. The second stage is related to the crystallization of hydroxide particles[30], while the last one originates from the carbonate species[2,28]. It seems that the presence of carbonate can affect the decomposition events of hydroxyl species, therefore, several exothermal peaks appear on the DTA curves. After digestion, the overall decomposition behavior of CeO_2-H80 is similar to that of CeO_2-C80, with a total weight loss of about 13% and an endothermic peak at around 60 ℃. This implies that the carbonate species has been hydrolyzed into hydroxyl species during the digestion.

2.2　Textural properties of CeO_2 samples

The surface area of the CeO_2 samples calcined at different temperatures is illustrated in Fig.6. As expected, the surface area decreases at higher temperatures, regardless of synthetic approaches [19]. However, the values are still appreciable. The surface area of CeO_2-H*t* is superior to that of CeO_2-C*t*. After calcination at 900 ℃, the surface area of the CeO_2-H*t* sample can be 27 $m^2 \cdot g^{-1}$, which is rather uncommon for pure CeO_2 material under such a harsh thermal treatment. This implies that the usage of ammonium carbonate hydrolysis approach allows the formation of CeO_2 with improved thermal stability.

Fig.7(a) and (b) display the nitrogen adsorption/desorption isotherms and the corresponding pore size distribution curves of the CeO_2-C500 and CeO_2-H500

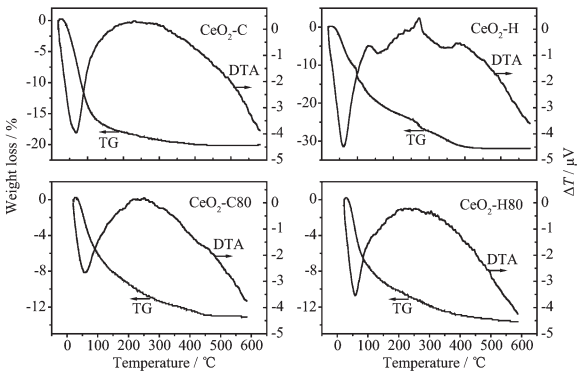

Fig.5　TG/DTA curves of precipitates

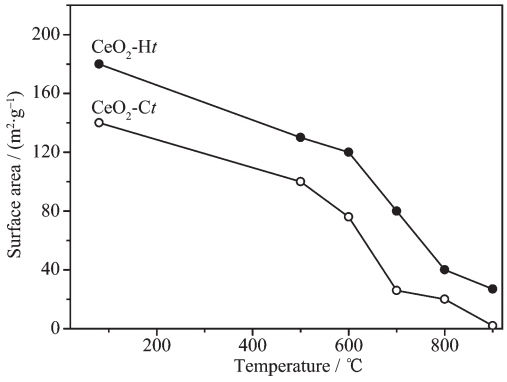

Fig.6　Surface area vs. calcination temperature

samples. According to the IUPAC definition, all the samples feature the isotherm of type Ⅳ, typical of a mesoporous material[42]. The shape of hysteresis loops indicates the presence of "ink-bottle" and cylindrical pores, which are favorable for gas and thermal diffusion[42]. Actually, the sintering behavior of CeO_2-based materials is strongly affected by the pore structure[43]. The pore size of CeO_2-H500 is larger than that of CeO_2-C500, which should be responsible for its improved thermal stability[5,36,44].

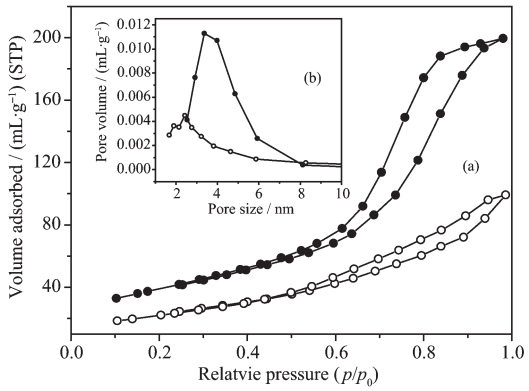

(○) CeO_2-C500; (●) CeO_2-H500

Fig.7 (a) N_2 adsorption-desorption isotherms of samples prepared by different methods; (b) Corresponding BJH pore size distribution curves

XRD patterns of the precipitates are shown in Fig.8. All the patterns show the diffraction peaks of CeO_2 with fluorite structure, regardless of preparation routes. The as-prepared samples, i.e., CeO_2-H and CeO_2-C, are also characterized by CeO_2, indicating that the hydrolysis event of carbonate species as well as the dehydration of hydroxyl groups has occurred before the heat treatment. Crystallite size of the precipitates is calculated using the (111) plane. The grain sizes of CeO_2-C (1.9 nm) and CeO_2-C80 (2.0 nm) are much smaller than those of CeO_2-H (3.9 nm) and CeO_2-H80 (4.0 nm). This suggests that the crystalline dimension depends on the synthetic routes. As for precipitation process, with progressively increasing concentration of the base solution, the mean magnitude of the individual crystal grain will decrease[45]. In the ammonia environment, The OH^- species in high concentration attacks Ce(Ⅳ) directly, resulting in a rapid nucleation rate. Consequently, uniformly small particles are obtained. However, in the case of ammonium carbonate, polymer of carbonate-containing precipitate, i.e., $Ce(O_2)(OH)_x(CO_3)_{1-x/2}$, can serve as a precursor of the CeO_2 oxide. The crystallization of CeO_2 proceeds through gradual hydrolysis of CO_3^{2-}, which inhibits the rate of precipitation and enlarges the crystallite size. However, after calcination at 500 ℃, the crystallite size of CeO_2-C500 (7.5 nm) becomes larger than that of CeO_2-H500 (4.2 nm). According to the literature[27], the primary particle of CeO_2-H is larger than that of CeO_2-C, which facilitates the formation of packing "ring" with larger pore space. Generally, the movement of coarsened particles of CeO_2-Ht is expected to be inhibited[44]. Moreover, the enlarged pores in CeO_2-Ht sinter with more difficulty as longer migration distance is needed for the matter to fill the pores[36]. Thus, the CeO_2 material prepared by ammonium carbonate-hydrolysis method is more thermally stable.

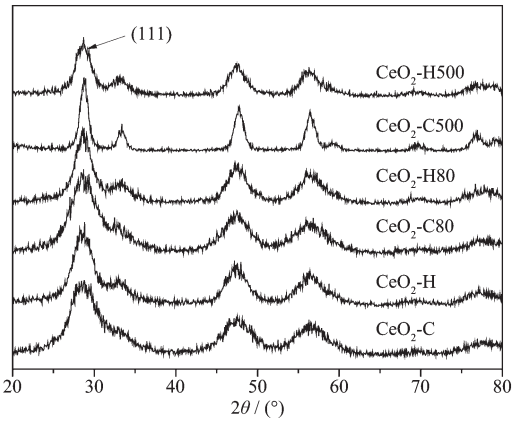

Fig.8 XRD parttens collected from precipitates

2.3 Reduction behavior of CeO_2 samples

A crucial requirement of CeO_2 material, especially when used as oxygen storage components for the purification of exhaust gases, is the reduction ability. Thus, the samples were calcined at 500 ℃ and 900 ℃, and then were employed to characterize the reduction behavior. From Fig.9, the reduction profiles of CeO_2-C500 and CeO_2-H500 consist of two peaks, which are ascribed to the reduction of surface and bulk oxygen species, respectively[46]. Although the outsets of the reduction peaks of the samples are almost the same, the integrated peak area of CeO_2-

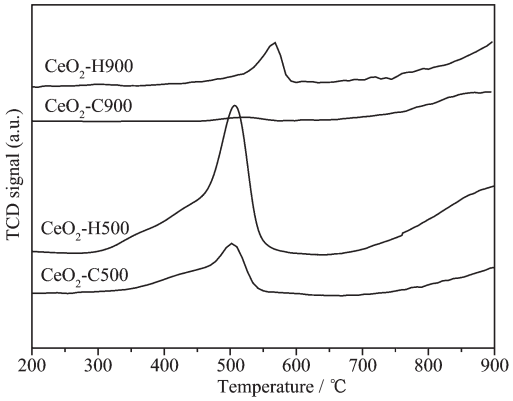

Fig.9　TPR profiles of CeO_2 samples

H500 is apparently larger than that of CeO_2-C500. This indicates that CeO_2-H500 is more reducible and active than CeO_2-C500[47]. The difference becomes more apparent after calcination at 900 ℃, especially in the low-temperature region.

3　Conclusions

In this work, CeO_2 oxide was prepared by a hydrothermal hydrolysis route using ammonium carbonate as the precipitant and hydrogen peroxide as the oxidizer. The title method was compared with the conventional method employing ammonia as the reactant. The formation mechanism of the precipitate was also studied. After digestion, the chemical compositions of the precipitates prepared by the two methods were almost the same. However, the crystallite size of the precipitates differs from each other greatly. The pore size of the as-prepared CeO_2 by the hydrolysis procedure is much larger, which facilitates the formation of CeO_2 oxide with improved textural and reduction properties. In particular, after calcination at 900 ℃ for 3 h, the CeO_2 powder from HA route still remains a surface area of 27 $m^2 \cdot g^{-1}$.

References:

[1] Matatov-Meytal Y I, Sheintuch M. *Ind. Eng. Chem. Res.*, **1998**,**37**(2):309-326

[2] Tikhomirov K, Krocher O, Elsener M, et al. *A. Appl. Catal. B*, **2006**,**64**(1/2):72-78

[3] Sahibzada M, Steele B C H, Zheng K, et al. *Catal. Today*, **1997**,**38**(4):459-466

[4] Kašpar J, Fornasiero P, Graziani M. *Catal. Today*, **1999**,**50**(2):285-298

[5] Di Monte R, Kašpar J, *Catal. Today*, **2005**,**100**:27-35

[6] Di Monte R, Fornasiero P, Kašpar J, et al. *Appl. Catal. B*: *Environ*., **2000**,**24**:157-167

[7] Kenevey K, Valdivieso F, Soustelle M, et al. *Appl. Catal. B*: *Environ*., **2001**,**29**:93-101

[8] Bueno-Lopez A, Such-Basanez I, de Lecea C S M. *J. Catal.*, **2006**,**244**(1):102-112

[9] Nagai Y, Hirabayashi T, Dohmae K, et al. *J. Catal.*, **2006**, **242**(1):103-109

[10]Perrichon V, Laachir A, Abouarnadasse S, et al. *Appl. Catal. A*, **1995**,**129**:69-82

[11]Hernández W Y, Laguna O H, Centeno M A, et al. *J. Solid State Chem.*, **2011**,**184**:3014-3020

[12]Karakoti A S, Kuchibhatla S V N T, Babu K S, et al. *J. Phys. Chem. C*, **2007**,**111**(46):17232-17240

[13]Ahniyaz A, Watanabe T, Yoshimura M. *J. Phys. Chem. B*, **2005**,**109**(13):6136-6139

[14]Si R, Zhang Y W, Wang L M, et al. *J. Phys. Chem. C*, **2007**,**111**(2):787-794

[15]Xian C N, Li H, Chen L Q, et al. *Micropor. Mesopor. Mat.*, **2011**,**142**:202-207

[16]Thammachart M, Meeyoo V, Risksomboon T, et al. *Catal. Today*, **2001**,**68**(1-3):53-61

[17]Fan J, Wu X D, Yang L, et al. *Catal. Today*, **2007**,**126**(3/4): 303-312

[18]Ni C Y, Li X Z, Chen Z G, et al. *Micropor. Mesopor. Mater.*, **2008**,**115**:247-252

[19]Terribile D, Trovarelli A, de Leitenburg C, et al. *Chem. Mater.*, **1997**,**9**(12):2676-2678

[20]Terribile D, Trovarelli A, Llorca J, et al. *J. Catal.*, **1998**,**178** (1):299-308

[21]Chen H R, Ye Z Q, Cui X Z, et al. *Micropor. Mesopor. Mater.*, **2011**,**143**:368-374

[22]Mokkelbost T, Kaus I, Grande T, et al. *Chem. Mater.*, **2004**, **16**(25):5489-5494

[23]Heo I, Choung J W, Kim P S, et al. *Appl. Catal. B*, **2009**,**92** (1/2):114-125

[24]Woodhead J L, *US Patent*, 4231893. 1980-11-04

[25]Scholes F H, Soste C, Hughes A E, et al. *Appl. Surf. Sci.*, **2006**,**253**(4):1770-1780

[26]Scholes F H, Hughes A E, Hardin S G, et al. *Chem. Mater.*, **2007**,**19**(9):2321-2328

[27]Chen P L, Chen I W. *J. Am. Ceram. Soc.*, **1997**,**80**(3):637-645

[28]Rebellato J, Natile M M, Glisenti A. *Appl. Catal. A*, **2008**,

339(2):108-120

[29]Li J G, Ikegami T, Mori T, et al. *Chem. Mater.*, **2001**,**13**(9):2913-2920

[30]Djuričić B, Pickering S. *J. Eur. Ceram. Soc.*, **1999**,**19**(11):1925-1934

[31]Binet C, Daturi M, Lavalley J C. *Catal. Today*, **1999**,**50**(2):207-225

[32]Natile M M, Boccaletti G, Glisenti A. *Chem. Mater.*, **2005**, **17**(25):6272-6286

[33]Lin W Y, Frei H. *J. Am. Chem. Soc.*, **2002**,**124**(31):9292-9298

[34]Klissurski D G, Uzunova E L. *Chem. Mater.*, **1991**,**3**(6):1060-1063

[35]Jobbagy M, Marino F, Schobrod B, et al. *Chem. Mater.*, **2006**,**18**(7):1945-1950

[36]Kašpar J, Fornasiero P. *J. Solid State Chem.*, **2003**,**171**(1/2):19-29

[37]Weng X L, Perston B, Wang X Z, et al. *Appl. Catal. B*: *Environ.*, **2009**,**90**:405-415

[38]Pushkarev V V, Kovalchuk V I, d′Itri J L. *J. Phys. Chem. B*, **2004**,**108**:5341-5348

[39]Zhang G J, Shen Z R, Liu M, et al. *J. Phys. Chem. B*, **2006**, **110**(51):25782-25790

[40]Alifanti M, Baps B, Blangenois N, et al. *Chem. Mater.*, **2003**,**15**(2):395-403

[41]Darnyanova S, Pawelec B, Arishtirova K, et al. *Appl. Catal. A*, **2008**,**337**(1):86-96

[42]Wang J, Wen J, Shen M Q. *J. Phys. Chem. C*, **2008**,**112**(13):5113-5122

[43]Rohart E, Larcher O, Deutsch S, et al. *Top Catal*, **2004**,**30-31**:417-423

[44]Kašpar J, Fornasiero P, Hickey N. *Catal. Today*, **2003**,**77**:419-449

[45]Von Weimarn P P. *Chem. Rev.*, **1925**,**2**(2):217-242

[46]Bruce L A, Hoang M, Hughes A E, et al. *Appl. Catal. A*, **1996**,**134**(2):351-362

[47]Masui T, Peng Y M, Machida K, et al. *Chem. Mater.*, **1998**, **10**(12):4005-4009